

# Detection and classification of Breast Cancer in Wavelet Sub-bands of Fractal Segmented Cancerous Zones

Alireza Shirazinodeh , Hossein Ahmadi Noubari<sup>1</sup>, Hossein Rabbani, Alireza Mehri Dehnavi

Department of Biomedical Engineering, Medical Image and Signal Processing Research Center, Isfahan University of Medical Sciences, Isfahan, Iran, <sup>1</sup>Department of Electrical and Computer Engineering, University of British Columbia, Vancouver, Canada

Submission: 29-05-2015

Accepted: 08-07-2015

## ABSTRACT

Recent studies on wavelet transform and fractal modeling applied on mammograms for the detection of cancerous tissues indicate that microcalcifications and masses can be utilized for the study of the morphology and diagnosis of cancerous cases. It is shown that the use of fractal modeling, as applied to a given image, can clearly discern cancerous zones from noncancerous areas. In this paper, for fractal modeling, the original image is first segmented into appropriate fractal boxes followed by identifying the fractal dimension of each windowed section using a computationally efficient two-dimensional box-counting algorithm. Furthermore, using appropriate wavelet sub-bands and image Reconstruction based on modified wavelet coefficients, it is shown that it is possible to arrive at enhanced features for detection of cancerous zones. In this paper, we have attempted to benefit from the advantages of both fractals and wavelets by introducing a new algorithm. By using a new algorithm named F1W2, the original image is first segmented into appropriate fractal boxes, and the fractal dimension of each windowed section is extracted. Following from that, by applying a maximum level threshold on fractal dimensions matrix, the best-segmented boxes are selected. In the next step, the segmented Cancerous zones which are candidates are then decomposed by utilizing standard orthogonal wavelet transform and db2 wavelet in three different resolution levels. After nullifying wavelet coefficients of the image at the first scale and low frequency band of the third scale, the modified reconstructed image is successfully utilized for detection of breast cancer regions by applying an appropriate threshold. For detection of cancerous zones, our simulations indicate the accuracy of 90.9% for masses and 88.99% for microcalcifications detection results using the F1W2 method. For classification of detected microcalcification into benign and malignant cases, eight features are identified and utilized in radial basis function neural network. Our simulation results indicate the accuracy of 92% classification using F1W2 method.

**Key words:** Algorithms, breast neoplasms, computer-assisted, fractals, image processing, mammography, neural networks, wavelet analysis

## INTRODUCTION

In 2013, an estimated 232,340 new cases of invasive breast cancer were expected to be diagnosed among US women, as well as an estimated 64,640 additional cases of *in situ* breast cancer. That year, approximately 39,620 US women were expected to die from breast cancer. Only lung cancer accounts for more cancer deaths in women.<sup>[1]</sup> It is also documented that early detection, diagnosis and treatment of illness can play a significant role in preventing mortality caused by cancer.<sup>[1]</sup> During recent years, considerable research has been carried out to reduce detection errors by applying some of the advanced image processing methods in the field of digital radiology. In our previous papers,<sup>[2,3]</sup> we used fractal modeling and wavelet transform for detection of microcalcifications, a comparative study analysis using probabilistic neural network, eight features

such as fractal dimension variations, entropy and wavelet coefficients were proposed to classify both malignant and benign cancerous zones. Gulsrud and Husoy<sup>[4]</sup> presented an effective CAD system based on the application of an optimal filter as a texture feature separator. By using a preprocessing technique based on spatial filters for enhancing signals, the characteristic extraction plan was applied on signals which included microcalcifications and normal tissues. For increasing the accuracy of performance, they used a large smoothing filter on post processed feature images. Liyang *et al.*<sup>[5]</sup> introduced a method based on relevance vector machine (RVM) to detect microcalcifications in digital mammograms. Furthermore, to increase the speed of the detection algorithm, they proposed a two-stage RVM classification method that non-MC pixels were eliminated by a faster linear RVM classifier. Higuera and co-workers<sup>[6]</sup> used the property of Gaussian models and produced a Bayesian

### Address for correspondence:

Dr. Hossein Rabbani, Department of Biomedical Engineering, Medical Image and Signal Processing Research Center, Isfahan University of Medical Sciences, Isfahan, Iran. E-mail: h\_rabbani@med.mui.ac.ir

classifier for the detection of microcalcifications in digital mammograms. By using the posterior probability estimation and an additional model selection algorithm based on prune, split and merge operations, they could show a significant relationship between entropic cost and area under the receiver operating characteristic curve. The main difference between malignant and normal cancerous cells is on the distribution and number of microclassifications. When a large number of microclassification cells form a dense mass clustered in a small area, they are categorized as malignant.<sup>[7]</sup> Masses in benign and malignant cases of mammograms have distinct and meaningful differences in terms of their shape and formation. In general cases, it seems that malignant tumors have irregular boundaries characterized with high and low-density contours where in cases of nonmalignant tumors, they have rather smooth boundaries with high and low oval type shape.<sup>[2,7]</sup> Beheshti *et al.*<sup>[8]</sup> presented a method for the detection and diagnosis of masses in digitized mammograms by using fractal modeling in two stages. First, they differentiated between masses and background tissues by using preprocessing techniques. Second, by applying the fractal dimension method, they could extract new fractal features to identify the roughness of the masses contours. Chang *et al.*<sup>[9]</sup> were able to classify tumors into benign and malignant types by using fractal Brownian motion to calculate the fractal dimension of ultrasound images, where they applied shape detection and K-means clustering algorithms for classification of tumors. In order to promote the classification performances, they applied morphology techniques and histogram equalizations on the ultrasound images as preprocessing methods. Öktem and Jouny<sup>[10]</sup> used fractal analysis and spatial moment distributions with the combination of back propagation neural network and a self-organizing map to classify unknown test mammograms into benign and malignant categories. In addition, they applied two-stage back propagation neural network and the one-stage self-organizing map to improve their study results. Nguyen and Rangayyan<sup>[11]</sup> used the fractal dimension based on shape analysis to classify the mammographic masses. They applied the box counting algorithm on mammograms and found that the fractal dimension may not be sensitive for detection of masses. Thus, they benefited the statistical measures of the texture of breast masses and tumors in a combination of fractal dimensions on gray scales mammograms to draw the shapes of tumors. Kontos *et al.*<sup>[12]</sup> showed that numerous types of breast cancer tissues tend to spread along the ductal lumen. They first calculated the fractal dimension containing ductal lumens and then they analyzed the fractal details of the ductal network in galactograms to detect early signs of cancerous tissues. Wavelets and wavelet transform have also been used as an independent framework of analysis in most of image processing applications. Lemaury *et al.*<sup>[13]</sup> produced a new wavelet algorithm with a higher regularity compare to the classical wavelets, then by using this new approach, they could improve the results of microcalcifications detections

in digitized mammograms. For this goal, the comparison algorithm was based on some features such as rate of correct detection, modulus of the wavelet coefficients, the rate of false alarm and number of detected spots. Heinlein *et al.*<sup>[14]</sup> used integrated wavelets to enhance the microcalcifications in digital mammograms. Their algorithm was gradually changing the image resolutions by converting scales given in millimeter-to-pixel resolutions. They could design a filter bank for decomposition and reconstruction without using slowly converging iterative plans. Finally, they showed that enhancement becomes more specific to microcalcifications. Nakayama *et al.*<sup>[15]</sup> used eight features based on the multi-resolution approach of the shape features, which were extracted by the enhancement of nodular components and linear nodular components. For more information, they proposed a new filter bank with high efficiency for the detection of microcalcifications clusters in mammograms. Mencattini *et al.*<sup>[16]</sup> used the dyadic wavelet transform as enhancement and denoising techniques for the preprocessing of microcalcifications and masses detection in digital mammograms. The main benefit of their method was adaptability to the different nature of diagnostic relevant features in the mammographic images. Karahaliou *et al.*<sup>[17]</sup> compared two classes of features which relate to the combination of gray level texture features and wavelet coefficient texture features to find a malignant underlying biological process. This paper tries to benefit from the advantages of both fractal and wavelet theories as a new algorithm named F1W2 is introduced in section II.E. In F1W2, the original image is segmented into appropriate fractal boxes, and the fractal dimension of each windowed section is extracted to detect the cancerous zones. Wavelet coefficients of the fractal segmented image at a first scale and low-frequency band of the third scale are set to zero. In section III, the performance of this algorithm is evaluated, and a few detection results are represented, as they were applied on various mammograms and compared with the proposed marked cancerous zones by a radiologist. Finally, this paper is concluded in section IV.

## MATERIALS AND METHODS

Mammograms used in this study are from MIAS (Mini Mammographic Database). The cancerous zones in this database are marked by radiologist by a single dot (as the center of the circle) and a circle around to identify the region. Furthermore, these mammograms, based on their background, are divided on to fatty, fatty-glandular, and dense-glandular; where from the point of view of being natural or not natural, they are classified into seven classes. In this study, we considered 127 mammograms consisting of mass cases which were used for detection of tumor lesions and microcalcification cases. We examined performance of our proposed hybrid approach using combination of fractal with wavelet which led to three algorithms, fractal analysis (section II. A), wavelet analysis (section II. B), and

combinations of fractal analysis and wavelet transform namely F1W2 (section II. C).

### Detection of Cancerous Zones Based on Fractal Dimension Analysis

In this section, we use a box-counting algorithm to extract the fractal dimension. This dimension gives an estimate of the space occupied by the fractal zone. In fractal zone analysis, assuming the size of the network cell is  $r$  and number of cells is  $n$ , if the area under the study is covered by a network of different sizes, then the cells of the network covering the image are assumed to increase without any bound in accordance with the following Eq. 1 after which fractal dimension is derived using following equation:

$$D_b = -\frac{\log n}{\log r} \quad (1)$$

In this method, an image is placed on a cross-word puzzle type grid having a cell size ranging from 1 to 100 pixels after which the number of cells that cover the entire image is counted as  $n$  regardless of the number of pixels in the cell. Then box counting is applied to the selected counted cells based on the algorithm used for cell size. This procedure is repeatedly applied to smaller size grid networks followed by counting number of cells  $n(r)$  that cover the given image. Slope of this line is fractal dimension of the image using the following formula:<sup>[2,7]</sup>

$$D = \frac{\log(n(r_2)) - \log(n(r_1))}{\log(r_2) - \log(r_1)} \quad (2)$$

However, noting that in real-world situations, images are rarely identical to each other, it is almost impossible to obtain a fractal dimension for the entirety of images. But we also note that there are similarities between images when localized sections in images are considered.<sup>[2,3]</sup> As such, a given image is segmented into smaller sections [Figure 1] and for each segment, fractal dimension is derived [Figure 2]. In Figure 3, the plot of  $\log(n)$  versus  $\log(r)$  for a segment of Figure 1 was shown where the average of the fractal array is the fractal dimension of this image segment. This is followed by averaging the fractal dimension of image segments and placing them into a matrix in accordance with the ordering used during the windowing for threshold purposes. At last, regions with maximal fractal dimension are identified as a cancerous zone.<sup>[3]</sup>

### Wavelet-based Cancerous Zones Detection

This section presents an algorithm for extraction of cancerous zones from mammograms using wavelet transform. Since wavelet transform classify features of image in different resolutions and noting that microcalcification and masses often reside in mid-range

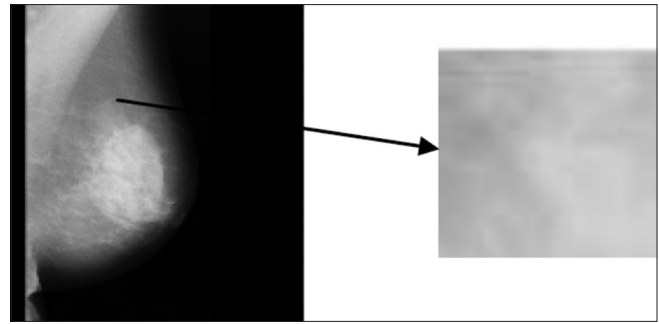


Figure 1: Left image: Original mammogram, Right: Expanded image segment

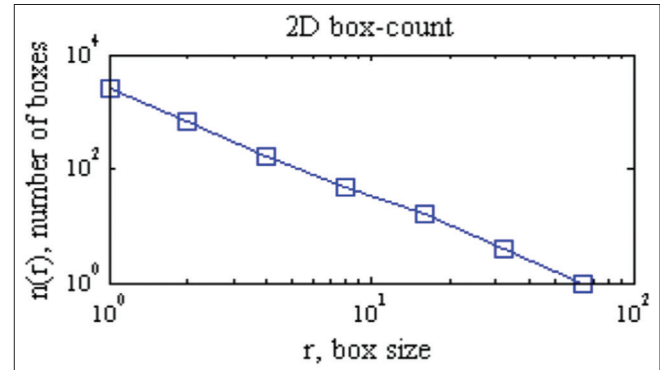


Figure 2: Plot of  $n$  and  $r$  of image segment of Figure 1

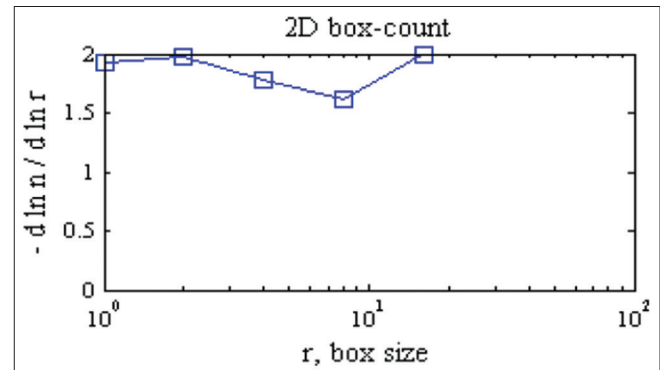


Figure 3: Logarithmic plot of fractal array

of resolution, it is possible to reconstruct image components that reside in medium scale range and as such to reconstruct image containing cancerous regions. At the first stage, an initial mammogram is analyzed in two distinct frequency bands using orthonormal wavelet transform in three different resolution levels. We used low order db2, which is suitable for detection of edges, as analyzing wavelets. Sub image of the low frequency band in third resolution contains information at the low frequency and mainly represents the background of a mammogram. However, sub-images of first resolution contain information about features that are of smaller dimensions as compared with microcalcification. For detection of microcalcification, it is necessary to nullify wavelet coefficients of the image at first scale as well as low frequency components at the third scale sub images,

whereby applying inverse transform on the remaining coefficients, reconstructed mammogram will have necessary information on medium frequency containing microcalcification. This is followed by applying a threshold to obtain the final results. Figure 4 shows sub-images of the first scale of a mammogram. In this figure, the texture of the mammogram can be clearly seen in low-frequency sub images while other sub-images contain information of high-frequency bands.<sup>[3]</sup>

### F1W2: Wavelet-based Cancer Detection in Images Extracted from Fractal Analysis

In this algorithm, at first the cancerous zone is extracted using fractal modeling (as described in section II. A) and then wavelet transform is used in a similar procedure explained in section II. B to produce a modified image for applying threshold operator. This method is implemented using the following steps:

- Extract the fractal dimension of each  $3 \times 3$  (overlapped) block of image and produce the fractal dimension matrix
- Apply a threshold on extracted matrix of step 1 and remove all coefficients smaller than threshold
- Apply db2 wavelet transform on produced image in the previous step (at three level resolutions)
- Nullify wavelet coefficients of the image at the first scale and low-frequency band of the third scale
- Apply inverse wavelet transform
- Apply Otsu's method threshold.

### Otsu's Method Threshold

In computer vision and image processing, Otsu's method is used to automatically perform clustering-based image threshold,<sup>[18]</sup> or, the reduction of a gray level image to a binary image. The algorithm assumes that the image contains two classes of pixels or bi-modal histogram then calculates the optimum threshold separating those two classes so that their combined spread (intra-class variance) is minimal.<sup>[19]</sup> The extension of the original method to the multi-level threshold is referred to as the multi-Otsu method.<sup>[20]</sup> In Otsu's method, we exhaustively search for the threshold that minimizes the intra-class variance (the variance within the class), defined as a weighted sum of variances of the two classes:

$$\sigma_w^2(t) = w_1(t)\sigma_1^2(t) + w_2(t)\sigma_2^2(t) \quad (3)$$

Weights  $w_i$  are the probabilities of the two classes separated by a threshold  $t$  and  $\sigma_i^2$  variances of these classes. Otsu shows that minimizing the intra-class variance is the same as maximizing inter-class variance:<sup>[18]</sup>

$$\sigma_b^2(t) = \sigma^2 - \sigma_w^2(t) = w_1(t)w_2(t)[\mu_1(t) - \mu_2(t)]^2 \quad (4)$$

Which is expressed in terms of class probabilities  $w_i$  and class means  $\mu_i$ , the class probability  $w_1$  is computed from the histogram as  $t$ :

$$w_1(t) = \sum_1^t p_i \quad (5)$$

While the class mean  $\mu_1$  is:

$$\mu_1(t) = [\sum_0^t p(i)x(i)] / w_1 \quad (6)$$

Where  $x(i)$  is the value at the center of the  $i^{\text{th}}$  histogram bin. Similarly,  $w_2(t)$  and  $\mu_2$  on the right-hand side of the histogram for bins greater than  $t$  can be computed, and the class probabilities and class means can be computed iteratively.

### Classification of Malignant and Benign Lesions

In previous sections, three methods were introduced for the identification of cancerous zones and detection of microcalcifications. Now these extracted images are utilized to extract several features including average of fractal dimensions and their variance, mean, variance, entropy, skewness, kurtosis, and index of dispersion of detection results where they are used as an input vector to probabilistic neural network classifier. Probabilistic neural networks can be used for classification problems in which the first layer computes distance from the input vector to the training vector where it produces a vector whose elements indicate how close the input to a training data is. The second layer sums these contributions for each class of inputs to produce as its output, a vector giving a probabilistic interpretation of proximity values. Finally, a complete transfer function on the output of the second layer selects the maximum of these probabilities and produces an integer value of 1 for that class and 0 for the other classes. For the probabilistic neural network, we have

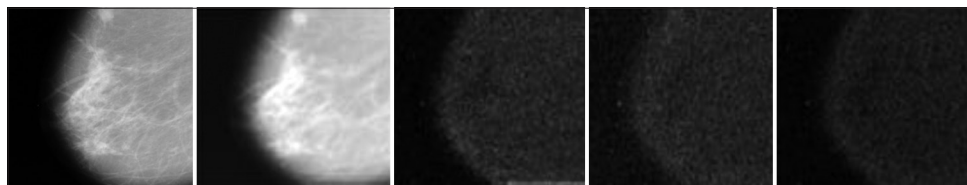


Figure 4: From left to right: original image, low frequency sub band of first scale, horizontal, vertical and diagonal sub bands of first scale of image

used the standard radial basis function in which Bayesian approach for density function estimation is utilized. Under this approach, input feature vectors are classified into two groups M (Malignant) or B (Benign). When an input vector belongs to a class such as M, the following probabilistic statement can be made using Bayesian estimation approach and classifier:

$$P_M C_M f_M(x) > P_B C_B f_B(x) \quad (7)$$

Where  $P_M$  is the probability of input features belonging to class M and  $C_M$  is the corresponding cost function.  $X_{Mi}$  shows  $i^{th}$  learning pattern belonging to class M,  $m_M$  is the number of learning patterns of class M, and  $\sigma$  is smoothing parameter (equivalent to the variance of Gaussian pdf). In probabilistic neural network, the following estimator is used to derive density function:<sup>[12]</sup>

$$f_x(x) = \frac{1}{(2\pi)^{\frac{n}{2}} \sigma^n} - \frac{1}{m_n} \sum_{i=1}^{m_n} \exp[-2 \frac{(x-x_x)^T (x-x_{xi})}{\sigma^2}] \quad (8)$$

The decision function for classification is given by:

$$Decision\ function = (f_M - f_B) > 0 \quad (9)$$

Where  $f_M(x)$  is the discriminate function for class M (Malignant), and  $f_B(x)$  is the discriminate function for class B (Benign). If the decision is  $>0$ , the unknown pattern  $x$  is assigned to class M; otherwise the unknown pattern is assigned to class B [Figure 5].

The first-layer “input weights<sub>1,1</sub>” are set to the transpose of the matrix formed from the number of input training pairs. When an input is presented to the “distance” box, it produces a vector whose elements indicate how close the input is to the vectors of the training set. These elements are multiplied element by element by the corresponding value of the bias term (first element) in Eq. 8. An input vector close to a training vector is represented by a number close to 1 in the output vector  $a^1$  [Figure 5]. If an input is close to several training vectors of a single class, it is represented by several elements of  $a^1$  that are close to 1. The second-layer weights are set to the matrix of target vectors. Each vector has  $a^1$  in one row only which is associated with that particular class

of input, and 0's elsewhere. Finally, the second layer transfer function as a competitive layer produces  $a^1$  corresponding to the largest elements and 0's elsewhere. Thus, the network has assigned the input vector into a class among the two, having the maximum probability value. As explained in previous sections, we used 102 mammograms in fractal approach (including 56 benign and 46 malignant) and in the other approach 25 mammograms (including 13 benign and 12 malignant) were used in classification of two groups into benign (benign and normal) and malignant (cancerous zone). We also used radiologist's decision on benignancy/malignancy tests which was considered as gold standard. The results of applying proposed methods are given in Table 1. In this table, classification of cancerous regions into benign or malignant are evaluated based on false negative (FN = true diagnosis of benign), true negative (TN = false diagnosis of benign), true positive (TP = true diagnosis of malignant)” and false positive (FP = false diagnostic of malignant) evaluation results. From these measures set of secondary parameters such as accuracy, sensitivity, specificity of the network, prediction evaluation of malignancy and prediction evaluation of benign are extracted. According to the results, the positive predictive value in wavelet method is higher than of fractal.

Method indicating the superiority of wavelet approach for detection of microcalcification in malignant cancers. This is for the reason that in fractal method distribution of malignant tissues are defined using probabilistic density function, whereas in wavelet method, we analyze mammograms in several scales that do not need to measure statistical distribution for detection of microcalcification. In fractal-based method study of the texture of mammograms, shape indicates benign cancers have certain shapes that are very small, and they appear as negative predictive value (NPV), and as such it is better than wavelet approach. Therefore in the nomination of PPN by fractal and wavelet parameters, we suggest to use fractal parameters with higher weight for detection of benign cancers and wavelet parameters with higher weight for detection of malignant cancers. From this table, it's clear that the combination of these methods leads to better results than using either of fractal-based or wavelet-based methods alone. This may be explained by noting the fact that fractal method is sensitive to tissue

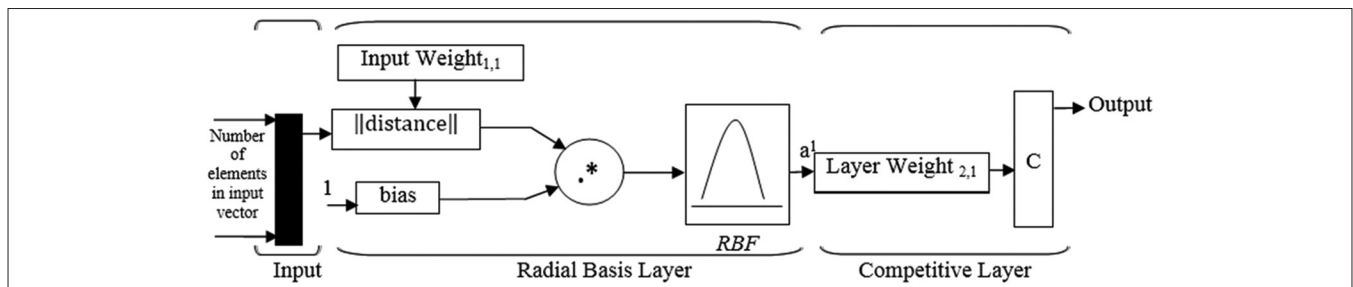


Figure 5: The general structure of probabilistic neural network

texture while wavelet transform is sensitive to edges of cancerous regions. As such combination of the fractal base method and wavelet transform results in a high success rate to differentiate the malignant lesion from benign ones.

## RESULTS

### Detection of Cancerous Zones

In this study, 127 mammograms, which were used for the detection of tumor lesions and microcalcifications, are selected for this study. The cancerous zones were marked by radiologist by a circle. Figure 6 shows sample malignant and benign images which to determine the fractal dimension, it is first divided into equal segments of size  $3 \times 3$ . Each of these images was of  $N_1 \times N_2$  pixels and  $N_3$  grayscale area.  $r$  and  $n$  are a collection of segments obtained from  $N_1 \times N_2$  pixels of the original image where  $r$  is a collection of disjoint cells and set  $n$  is a collection of cells not contained in  $r$ . The fractal dimension of different regions is then calculated using Eq. 2 and after applying a threshold, they are segmented from the original image and placed on the original image. Note that based on choosing the threshold value we were able to obtain both cancerous zones and microcalcifications. Figure 7 shows results of applying the F1W2 method as discussed in section II. C,

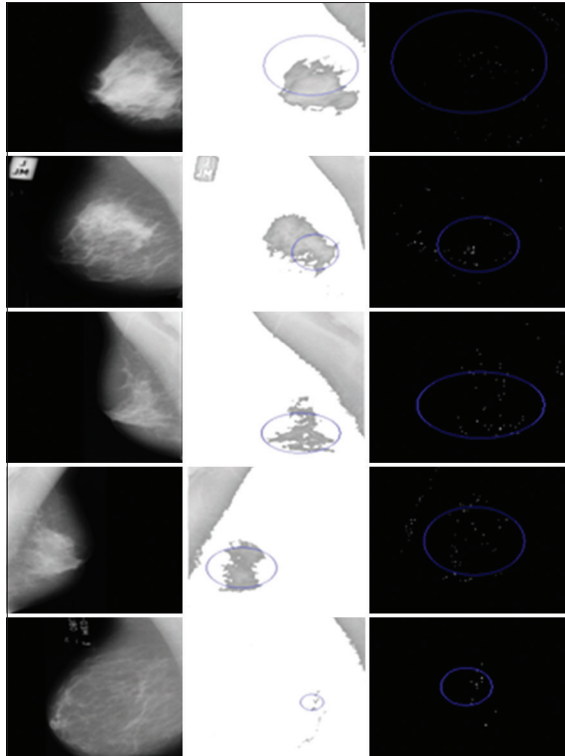


**Figure 6:** Detection of microcalcifications and cancerous zones by F1W2 method in sample images from MIAS database, original images (left column, from top to bottom: mdb001, mdb209, mdb213, mdb214, mdb231), Segmented regions using Fractal method, (middle column), Detected microcalcifications and cancerous zones by F1W2 approach (right column)

for extracting microcalcifications and cancerous zones in sample images. The results shown in the circle are defined by radiologists who marked them as microcalcification and cancerous zones.

### Thresholding of Intensity Levels

In this section, we examine the effect of the threshold of intensity levels on the detection results by using wavelet sub-bands as applied on fractal boxes images derived from fractal modeling algorithm. The main reason to apply the maximum level threshold on fractal dimension of matrix, which is related to  $3 \times 3$  blocks of original images, comes back to box-counting algorithm that we have used for the detection and segmentation of cancerous zones. According to the fractal theory, we have to consider the truth that the complexity of the boundaries is exactly related to the fractal dimension of images, and hence it is rather rational to accept this concept that some regions with regular shapes and smooth boundaries have the lower fractal dimension means than others. On the other hand, in contrast to breast tissues, the cancerous regions that involve cancerous regions have irregular boundaries with high-level gray scales in mammograms. Thus according to the formula 3, these regions have a greater fractal dimension than none cancerous regions as such grounds cause us to choose the maximum level of the threshold for the segmentation of the cancerous regions candidates. After the separation of cancerous blocks with the fractal algorithm and the application of wavelet transform, we apply Otsu's threshold to detect cancerous zones and determine the quantity of their variance. We consider that the cancerous zones have higher gray scale level than other regions; therefore, we nullify regions, which have lower gray scales in contrast to Otsu's threshold level. Table 2 shows that three characteristics of features of sensitivity, specificity and accuracy for all cases which examined in light of the change in the threshold level for detection of cancerous zones. In this table, detection of cancerous regions are evaluated based on FN (false diagnosis of noncancerous zones), TN (true diagnosis of noncancerous zones), TP (true diagnosis of cancerous zones) and FP (false diagnostic of cancerous zones) evaluation results. From these measures set of secondary parameters such as accuracy, sensitivity and specificity of the detection results are extracted. Measurements results in Table 1 indicate the extent to which detected regions by the radiologist are compatible with those of selected by the algorithm. In fractal detection and segmentation, we note that Max threshold is not selected manually, where it is determined based the algorithm in which the mean of fractal dimension of each of the blocks of original image is determined and compared with other blocks means. If the integer values of the mean are more than or equal to those belonging to neighboring blocks, this block is selected as a candidate block.

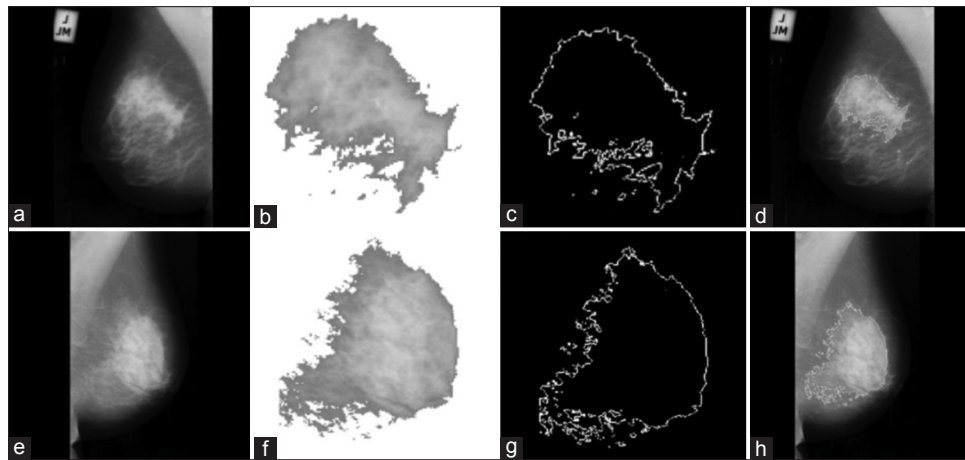


**Figure 7:** Segmentation of cancerous regions by fractal modeling for a malignant (top row) and benign images (bottom row), (a and e) original images (mdb209, mdb212), (b and f) detected region using fractal-based method, (c and g) cancerous region boundary, (d and h) locating cancerous regions on the original images

**Table 1:** Performance of three different methods and classification results using the output of probabilistic neural network

	Method		
	Fractal-based	Wavelet-based	FIW2
Accuracy	76	80	92
Sensitivity	81.81	83.34	92.31
Specificity	71.34	76.93	91.67
Malignancy prediction evaluation	69.23	76.93	92.31
Benignancy prediction evaluation	83.34	83.34	91.67

$$\text{Accuracy} = \frac{TP + TN}{TP + TN + FP + FN}, \text{Sensitivity} = \frac{TP}{TP + FN}, \text{Specificity} = \frac{TN}{TN + FP}$$

$$\text{PEM} = \frac{TP}{TN + FP}, \text{PEB} = \frac{TN}{TN + FN}$$

**Table 2:** Illustration of characteristic features of sensitivity, specificity and accuracy as influenced by selection of Otsu's method and maximum level threshold under FIW2 approach

Case	Specificity	Sensitivity	Accuracy
Masses	0.3218	0.9614	0.8911
Microcalcifications	0.3189	0.8917	0.8899

$$\text{Accuracy} = \frac{TP + TN}{TP + TN + FP + FN}, \text{Sensitivity} = \frac{TP}{TP + FN}, \text{Specificity} = \frac{TN}{TN + FP}$$

## CONCLUSION

The use of the FIW2 seems to be a rather sophisticated approach for the detection of microcalcifications and cancerous zones since by applying FIW2 in mammograms; we can benefit from both fractal modeling and multi-resolution wavelet transform techniques. Basically, fractal modeling of images and the extraction of the sub-images with higher fractal dimension rather than other sub-images are important by focusing on the texture of original images

and searching between depths of pixels with various gray scale levels to detect the complex textures. This method is efficient, considering that we could select the regions with a high probability of details and some information about cancerous zones in contrast to breast tissues which are normal. By reviewing the detection and segmentation fractal modeling results [Figure 6], we can recognize that the fractal modeling of images are not related to the arrangement of microcalcifications or their structures as this method only detects the boundary of sub-images that are candidates for cancerous regions. But details are important, and we should detect the concentration of cancerous zones that fractal modeling did not give us an overview about their structures or variances. At this stage, decomposition of fractal sub images with wavelet transform to subband images in different resolutions can be significant approaches that we have represented in this article (FIW2). By using these techniques, we can explore the cancerous zones' structures and arrangements to be able to use the results of such benefits to classify these cancerous regions to benign and normal or malignant cases in the next article. However, the FIW2 is a powerful approach since via wavelet transform on fractal segmented sub-images, we can reduce noises by nullifying the coefficient of high-frequency scales at the first level of decomposition; likewise, we can remove the background by nullifying the coefficient which is related to the sub-images of low-frequency scales at the third level decomposition. Hence, we can reconstruct a new image according to our changes to detect the arrangement of cancerous zones' structures and increase the efficiency of our algorithm. The results which are related to the FIW2 detection approach are shown in Figure 7.

## REFERENCES

1. American Cancer Society. Cancer Facts and Figures 2013. Atlanta: American Cancer Society; 2013, 2014.

2. Shirazinodeh A, AhmadiNoubari H, Mehridehnavi A, Rabbani H. Application of Wavelets and Fractal-based Methods for Detection of Microcalcification in Mammograms, A Comparative Analysis Using Neural Network. In ICSIP; 2010. p. 687-92.
3. Shirazinodeh A, Rabbani H, Mehridehnavi A, AhmadiNoubari H. "Detection of Cancerous Zones in Mammograms Using Fractal Modeling and Classification by Probabilistic Neural Network", Indexed in IEEE Section, Proceedings of the 17<sup>th</sup> Iranian Conference on Biomedical Engineering, ICBME; 2010. p. 2010.
4. Gulsrud T, Husøy J. Optimal filter-based detection of microcalcifications. *IEEE Trans Biomed Eng* 2001;48:1272-81.
5. Wei L, Yang Y, Nishikawa RM, Wernick MN, Edwards A. Relevance vector machine for automatic detection of clustered microcalcifications. *IEEE Trans Med Imaging* 2005;24:1278-85.
6. Higuera P, Arribas J, Moreno E, Lopez C. "A Comparative Study on Microcalcification Detection Methods with Posterior Probability Estimation Based on Gaussian Mixture Models," Proceedings of the 2005 IEEE Engineering in Medicine and Biology 27<sup>th</sup> Annual Conference, Shanghai, China; September 1-4, 2005.
7. Li H, Liu KJ, Lo SC. Fractal modeling and segmentation for the enhancement of microcalcifications in digital mammograms. *IEEE Trans Med Imaging* 2002;16:785-98.
8. Beheshti SMA, AhmadiNoubari H, Fatemizadeh E, Khalili M. An efficient fractal method for detection and diagnosis of breast masses in mammograms. *J Digit Imaging* 2014;27:661-9.
9. Chang R, Chen C, Ho M, Chen D, Moon W. "Breast Ultrasound Image Classification Using Fractal Analysis," Proceedings of the Fourth IEEE Symposium on Bioinformatics and Bioengineering (BIBE'04); 2004.
10. Öktem V, Jouny I. "Automatic Detection of Malignant Tumors in Mammograms," Proceedings of the 26<sup>th</sup> Annual International Conference of the IEEE EMBS, San Francisco, CA, USA; September 1-5, 2004.
11. Nguyen T, Rangayyan R. "Shape Analysis of Breast Masses in Mammograms via the Fractal Dimension," Proceedings of the 2005 IEEE Engineering in Medicine and Biology 27<sup>th</sup> Annual Conference, Shanghai, China; September 1-4, 2005. p. 3210-3.
12. Kontos D, Megalooikonomo V, Javadi A, Bakic P, Maidment A. "Classification of Galactograms Using Fractal Properties of the Breast Ductal Network," 3<sup>rd</sup> IEEE International Symposium on Biomedical Imaging: Nano to Macro, Arlington, VA; April 6-9, 2006.
13. Lemaire G, Drouiche K, DeConinck J. Highly regular wavelets for the detection of clustered microcalcifications in mammograms. *IEEE Trans Med Imaging* 2003;22:393-401.
14. Heinlein P, Drexler J, Schneider W. Integrated wavelets for enhancement of microcalcifications in digital mammography. *IEEE Trans Med Imaging* 2003;22:402-13.
15. Nakayama R, Uchiyama Y, Yamamoto K, Watanabe R, Namba K. Computer-aided diagnosis scheme using a filter bank for detection of microcalcification clusters in mammograms. *IEEE Trans Biomed Eng* 2006;53:273-83.
16. Mencattini A, Salmeri M, Lojacono R, Frigerio M, Caselli F. Mammographic images enhancement and de noising for breast cancer detection using dyadic wavelet processing. *IEEE Trans Instrum Meas* 2008;57:1422-9.
17. Karahaliou AN, Boniatis IS, Skiadopoulos SG, Sakellaropoulos FN, Arikidis NS, Likaki EA, et al. Breast cancer diagnosis: Analyzing texture of tissue surrounding microcalcifications. *IEEE Trans Inf Technol Biomed* 2008;12:731-8.
18. Sezgin M, Sankur B. Survey over image thresholding techniques and quantitative performance evaluation. *J Electron Imaging* 2004;13:146-65.
19. Otsu N. A threshold selection method from gray-level histograms. *IEEE Trans Syst Man Cybern* 1979;1:62-6.
20. Liao P, Chen T, Chung P. A fast algorithm for multilevel thresholding. *J Inf Sci Eng* 2001;17:713-27.

**How to cite this article:** Shirazinodeh A, Noubari HA, Rabbani H, Dehnavi AM. Detection and classification of Breast Cancer in Wavelet Sub-bands of Fractal Segmented Cancerous Zones. *J Med Sign Sence* 2015;5:162-70.

**Source of Support:** Nil, **Conflict of Interest:** None declared



## BIOGRAPHIES



**Alireza Shirazinodeh** is a PhD student of Biomedical Engineering at Tehran University of Medical Science. He has two Msc degrees, first in Biomedical Engineering from Isfahan University of Medical Sciences and second in Electrical Engineering and control Systems from Science and Research branch of Azad University. His area of interest include Image processing, Fractal theory and wavelet transform.

**E-mail:** a-shirazinodeh@razi.tums.ac.ir



**Hossein Ahmadi Noubari** is Professor Emeritus, Department of Electrical and Computer Engineering, University of Tehran, Iran and adjunct Professor at the Dept. of Electrical and Computer Engineering, University of British Columbia, Canada. He has held several research positions including visiting scholar at Academy of Science, China as well as visiting professor position at Stanford University and University of California, Berkeley. Author has also held several faculty positions in USA including assistant and associate professor at Polytechnic Institute of New York and Fairleigh Dickenson University. His area of interest include control systems modeling as applied to biomedical Engineering problem. He is founder of Control Systems and Instrument Engineering Society of Iran. His academic and research work during last ten years has been on wavelets and process modeling as applied to biomedical as well as industrial signal processing problems.

**E-mail:** noubari@ece.ubc.ca



**Hossein Rabbani** received the B.Sc. degree in Electrical Engineering (Communications) from Isfahan University of Technology, Isfahan, Iran, in 2000 with the highest honors, and the M.Sc. and Ph.D. degrees in Bioelectrical Engineering in 2002 and

2008, respectively, from Amirkabir University of Technology (Tehran Polytechnic), Tehran, Iran. In 2007 he was with the Department of Electrical and Computer Engineering, Queen's University, Kingston, ON, Canada, as a Visiting Researcher, in 2011 with the University of Iowa, IA, United States, as a Postdoctoral Research Scholar, and in 2013-2014 with Duke University Eye Center as a Postdoctoral Fellow. He is now an Associate Professor in Biomedical Engineering Department and Medical Image & Signal Processing Research Center, Isfahan University of Medical Sciences, Isfahan, Iran. Dr. Rabbani is a Senior Member of IEEE (Signal Processing Society, Engineering in Medicine and Biology Society, Circuits and Systems Society, Computer Society), and Editor-in-Chief of Journal of Medical Signals and Sensors. His main research interests are medical image analysis and modeling, statistical (multidimensional) signal processing, sparse transforms, and image restoration, which more than 110 papers and book chapters have been published by him as an author or co-author in these areas.

**E-mail:** h\_rabbani@med.mui.ac.ir



**Alireza Mehri Dehnavi** was born in Isfahan province at 1961. He had educated in Electronic Engineering at Isfahan University of Technology at 1988. He had finished Master of Engineering in Measurement and Instrumentation at Indian Institute of Technology Roorkee (IIT Roorkee) in India at 1992. He has finished his PhD in Medical Engineering at Liverpool University in UK at 1996. He is an Associate Professor of Medical Engineering at Medical Physics and Engineering Department in Medical School of Isfahan University of Medical Sciences. He is currently visiting at School of Optometry and Visual Science at University of Waterloo in Canada. His research interests are medical optics, devices and signal processing.

**E-mail:** mehri@med.mui.ac.ir